Comput Geosci (2008) 12:491–501
DOI 10.1007/s10596-008-9088-8

ORIGINAL PAPER

Artificial neural network and liquefaction susceptibility assessment: a case study using the 2001 Bhuj earthquake data, Gujarat, India

D. Ramakrishnan · T. N. Singh · N. Purwar · K. S. Barde · Akshay. Gulati · S. Gupta

Received: 9 June 2007 / Accepted: 17 April 2008 / Published online: 25 June 2008
© Springer Science + Business Media B.V. 2008

Abstract This study pertains to prediction of liquefaction susceptibility of unconsolidated sediments using artificial neural network (ANN) as a prediction model. The backpropagation neural network was trained, tested, and validated with 23 datasets comprising parameters such as cyclic resistance ratio (CRR), cyclic stress ratio (CSR), liquefaction severity index (LSI), and liquefaction sensitivity index (LSeI). The network was also trained to predict the CRR values from LSI, LSeI, and CSR values. The predicted results were comparable with the field data on CRR and liquefaction severity. Thus, this study indicates the potentiality of the ANN technique in mapping the liquefaction susceptibility of the area.

Keywords Liquefaction susceptibility · Neural network · Bhuj

1 Introduction

The January 26, 2001 Bhuj earthquake (M_w 7.6) in western India was one of the most devastating seismic events to affect the state since 1819 (M_w 7.7). The epicenter of the main shock of the event was located near Bachau at latitude 23.36° N and longitude 70.34° E with focal depth of about 23.6 km. In the entire Bhuj peninsula, liquefaction-related ground failures such as lateral spreads, sand boils, and flow slides resulted in severe damages to structures built on alluvium [1–3]. The seismically active Kachchh region has witnessed several devastative earthquakes in the recent history [4]. Still, microseismic zonation (MSZ) of this area is in rudimentary stage. Liquefaction susceptibility, one of the key components of MSZ, was evaluated by several earlier workers based on geotechnical parameters [1–3], site response [5], and co-seismic liquefaction severity [6].

Artificial neural network (ANN) is a soft computing approach which is being used around the globe to find solutions to a wide variety of non-linear problems. Neural network has the ability to learn from the pattern acquainted before. Once the network has been trained with sufficient number of sample datasets, it can make predictions, on the basis of its previous learning about the output related to new input dataset of similar pattern [7]. Due to its multidisciplinary nature, ANN is becoming popular among the researchers, planners, designers, etc., as an effective tool for the accomplishment of their work. ANN models have also been used in the field of geotechnical engineering. Goh [8, 9] developed backpropagation neural network (BPNN) models to evaluate the shaft resistance of piles driven in cohesive soil. Teh [10] developed a BPNN model to estimate the static pile capacity from the dynamic stress wave data. Neural network is also gaining importance in liquefaction susceptibility evaluation of foundation soils [11–13].

D. Ramakrishnan · T. N. Singh (✉) · Akshay. Gulati
Department of Earth Sciences,
Indian Institute of Technology,
Powai, Mumbai 400 076, India
e-mail: tnsingh@iitb.ac.in

N. Purwar · K. S. Barde · S. Gupta
Institute of Technology, Banaras Hindu University,
Varanasi 221 005, India

In this paper, the details pertaining to the January 26, 2001 event-induced liquefaction such as liquefaction severity index (LSI), liquefaction sensitivity index (LSeI), cyclic stress ratio (CSR), and cyclic resistance ratio (CRR) were taken, and an ANN model (BPNN) was developed to predict the liquefaction susceptibility. Here, two neural networks have been used; the first network was used to evaluate the CRR values from the established relation among CSR, LSI, and LSeI. For this purpose, the network was trained, tested, and validated with 23 datasets. The second network was used for predicting the liquefaction susceptibility of alluvium by taking the relationship among CRR, CSR, LSeI, and LSI.

2 Liquefaction susceptibility/severity criteria

2.1 Geotechnical criteria

Liquefaction generally occurs in areas with geologically young (Holocene to late Pleistocene) unconsolidated sediments comprising gravel, sand, and silt with high ground water levels [14–17]. Common surface manifestations of soil liquefaction include sand boils, differential settlements, flow slides, lateral spreading, and loss of bearing strength of foundation soils. Such ground failures result in damage to buildings, dams, bridges, and other military/civilian facilities. The risk of liquefaction and associated ground deformation can also trigger to additional hazards such as landslides and dam burst [15].

Liquefaction susceptibility of the alluvial area is evaluated from the point of *demand*, *capacity*, and *factor of safety*. Liquefaction demand is the load imparted to the soil by earthquake (in terms of both amplitude and duration). Capacity is the demand required to cause liquefaction, and factor of safety is the ratio between the capacity and demand. Liquefaction of saturated, unconsolidated sand, loam, and gravel occurs when the demand is more than the capacity. The liquefaction susceptibility of a foundation soil is evaluated on the basis of information on sediment type, depth to water table, seismic load, and resistance of the soil [18]. Liquefaction susceptibility of recent alluvial materials was generally evaluated from field data on cyclic stress ratio and cyclic resistance ratio [19, 20]. The resistance to liquefaction (CRR) of the foundation soil was evaluated using the field data on standard penetration test (SPT), in situ density, and soil index properties [20, 21]. These data were evaluated following the Indian Standard procedures (IS: 2131-1981). Normalization and corrections for the SPT values were carried out following the procedures prescribed by Youd et al. [19].

For evaluating the CRR values, filed SPT were conducted at 13 sites in and around Bhuj city. Select data pertaining to lithology, fine content, field density, and penetration resistance (SPT) are evaluated (Fig. 1, Table 1). The field SPT values are normalized to 100 kPa overburden pressure and 60% hammer efficiency $(N_1)_{60}$. The earthquake load measured through CSR is evaluated from the simplified procedures of

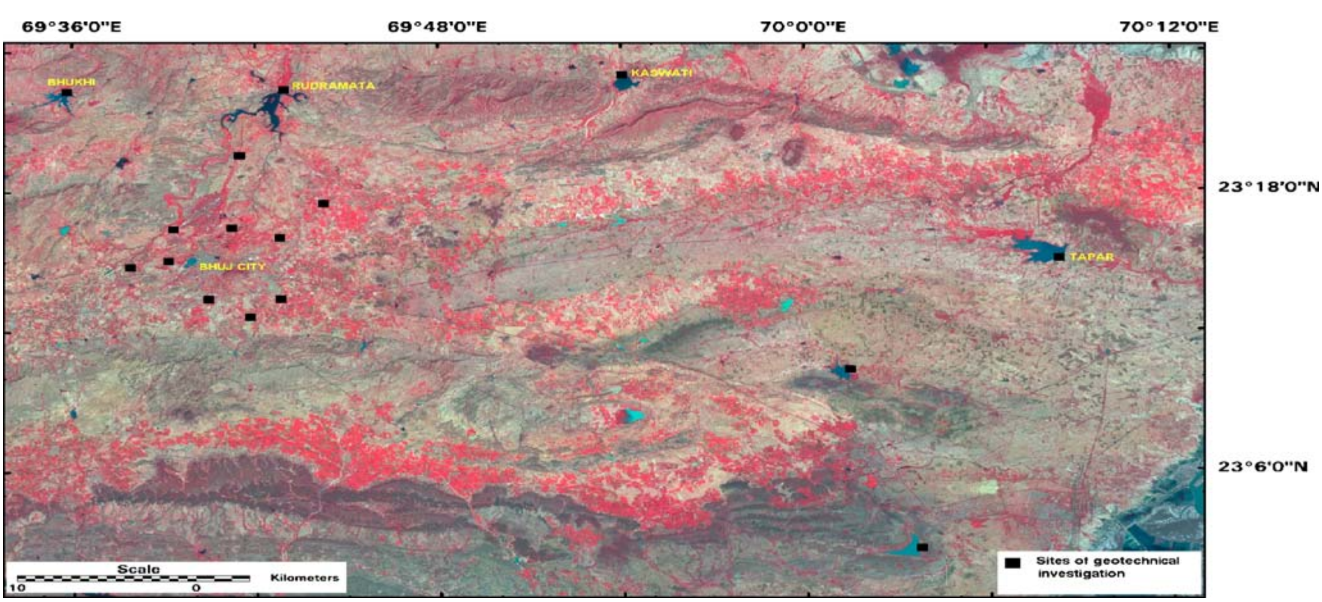

Fig. 1 Standard FCC of the Bhuj region depicting the sites of geotechnical studies pertaining to liquefaction susceptibility of sediments

Table 1 Select borehole records depicting the lithology, SPT, and index properties of soils

Bore hole no.	Location	Depth (m)	Lithology	Fines (%)	Soil class	SPT ($N_{1,60}$)	Density (%)	RWL (m)
BH1	Madhapar	< 1	Silty sand	12	SP–SM	14	40	18.0
		1–5	Coarse sand with pebbles	5	SP	16	35	
		5–7	Silty sand with clay	27	SM	25	65	
BH2	North of Bhuj town	< 1	Bentonitic clay and sand	30	SM	15	30	17.4
		1–2	Weathered S.St.	N.A.	N.A.	49	95	
		2.5	Weathered S.St.	N.A.	N.A.	N.A.	N.A.	
BH3	East of Bhuj town	< 1	Silty sand and coarse sand	6	SM	11	33	22.5
		1–3	Coarse sand	3	SP	12	37	
		3–5	Medium–fine sand	11	SP	24	60	
BH5	Airport	< 1	Coarse sand with clay	14	SP–SC	12	25	12.0
		1–2	Sand with clay	11	SP	32	65	
		2–7	Coarse sand	6	SP	39	60	
BH6	Rawal Wadi	< 2	Silty sand	7	SM	16	42	19.4
		2–4	Coarse sand	4	SP	7	23	
		4–8	Coarse sand with clays	24	SP–SC	45	87	
BH7	Haripar	< 1	Coarse sand with silt	8	SP	15	56	30.0
		1–3	Fine sand with silt	5	SM	21	37	
		3–5	Coarse sand with clay	11	SP	30	68	
BH8	Mirzapur	< 1	Silty sand	12	SM	28	35	22.5
		1–2	Coarse sand	5	SP	7	40	
		2–6	Silty sand	11	SP–SM	13	48	
		6–9	Weathered S.St.	N.A.	N.A.	49	89	
BH9	Near Bhuj cantonment	< 1	Silty sand	14	SM	24	46	25.0
		1–2	Coarse sand with silt	7	SP	24	68	
		2–3	Weathered S.St	N.A.	N.A.	39	84	
BH10	Ghenla	< 1	Coarse sand with clay	21	SP–SC	10	32	13.2
		1–2	Fine sand with silt, gravel	15	SP	15	47	
		2–6	Coarse sand	11	SP	29	55	
		6–7	Weathered S.St	N.A.	N.A.	36	85	
BH12	Parishram tower	< 1	Coarse sand	6	SP–SM	16	35	8.2
		1–3	Silty sand	13	SM	27	65	
		3–5	Sand	16	SP	46	89	
		> 5	Weathered S.St.	N.A.	N.A.	N.A.	N.A.	
BH13	Airport road	< 1	Coarse sand with clay	12	SP–SC	12	30	21.0
		1–3	Silty sand	9	SM	26	57	
		3–4	Sand with clays	15	SP	23	40	
		4–9	Clayey sand	24	SC	17	67	

N.A. = Not Available; S.St = Sand Stone

Seed and Idriss [20] for Peak Ground Acceleration (PGA) varying between 0.36 and 0.38. Besides these generated datasets, published datasets [1, 3] are also used in this study for training the network (Table 2).

2.2 Liquefaction severity criteria

LSI is a widely accepted quantitative measure of liquefaction severity [22]. The LSI values derived for the

Table 2 Set of input parameters of earthquake-affected area

Serial no.	Location	CSR	LSI	LSeI	CRR	Liquefaction susceptibility (1='YES'; 2='No')	BPNN
Summary of training data							
1	Madhapur	0.25	20	0.38	0.22	1	1.0001
2	N. Bhuj TN.	0.23	5	2.277	0.25	1	1.0002
3	E. Bhuj TN.	0.26	2	2.706	0.38	2	2.0003
4	Airport	0.23	10	1.6	0.22	1	1.0002
5	Bhuki	0.277	30	−1.43	0.325	2	2.0003
6	Kaswati	0.385	50	−2.2	0.325	1	1.0002
7	Suvi	0.466	60	−2.67	0.325	1	1.9998
8	N.Bhuj Cant.	0.24	5	3.521	0.27	1	1.0002
9	Ghenla	0.25	2	2.606	0.33	2	2.0003
10	Parishram	0.25	7	2.428	0.22	1	1.0002
11	Airport Road	0.23	20	0.351	0.21	1	1.0002
12	Mirzapur	0.26	2	3.015	0.34	2	2.0001
Summary of testing data							
13	Rawalwadi	0.23	10	1.6	0.22	1	1
14	Rudramata	0.389	50	−2.23	0.325	1	1.0002
15	Haripar	0.25	5	2.312	0.32	2	2.0001
16	Chang	0.73	70	−2.27	0.32	1	1.0003
17	Shivlakha	0.63	50	−5	0.32	1	1.4237[a]
Summary of validation data							
18	Bhuj (airport)	0.274	15	1.62	0.2603[b]	1[c]	1.0001[d]
19	Lodai	0.3288	60	−2.17	0.2462[b]	1[c]	1[d]
20	Chobari-I	0.274	40	−1.71	0.3105[b]	2[c]	1.8256[d]
21	Manfara	0.274	20	1.3	0.2333[b]	1[c]	1.0001[d]
22	Angar	0.328	5	2.09	0.3626[b]	2[c]	1.9999[d]
23	Litle Rann	0.274	50	−1.96	0.2735[b]	1[c]	1.0001[d]

[a] Architectural error
[b] Calculated value of CRR
[c] Inferred liquefaction susceptibility
[d] Predicted liquefaction susceptibility

Fig. 2 LSI–LSeI correlations for the Bhuj earthquake 2001

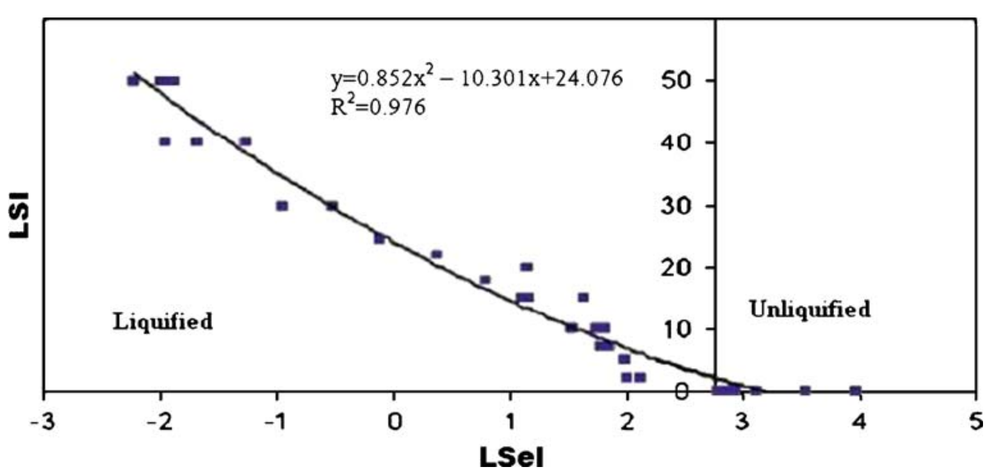

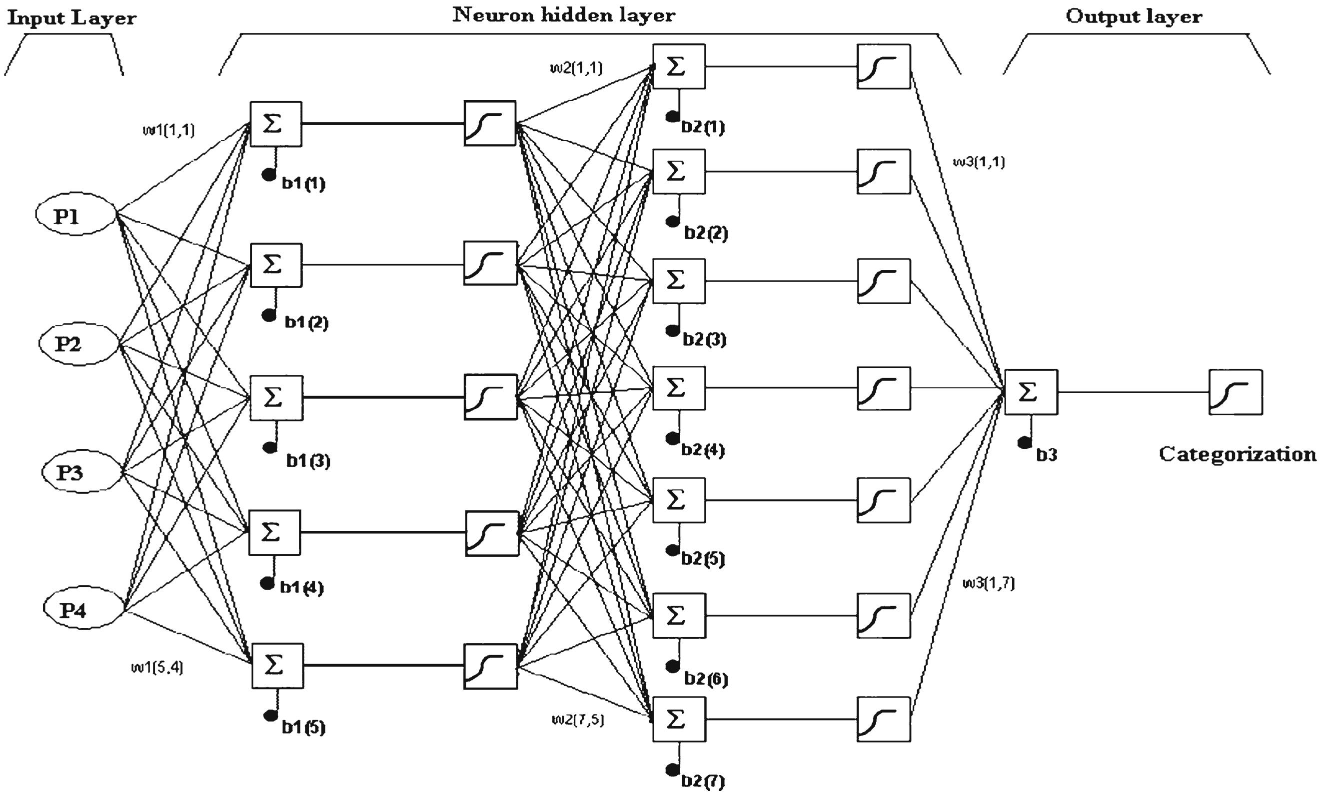

Fig. 3 Network architecture for predicting liquefaction susceptibility

2001 event with a magnitude of 7.7 and epicenter distance up to 100 km yielded a LSI range between 2 and 60. Liquefaction sensitivity index is a new technique in evaluating the severity from multi/hyperspectral satellite data [6]. It involves measurement of radiant energy of the earthquake affected areas in NIR and SWIR regions of electromagnetic radiation (EMR). Since these regions of EMR are sensitive to soil moisture, the liquefied regions show strong absorption of energy. The extent of absorbance is directly proportional to the degree of liquefaction severity. It was found that the LSeI and LSI values for the 2001 event have a strong correlation ($R^2 = 0.97$; Fig. 2). Further, the geotechnical criteria (CSR, CRR) also commensurate well with observed severity criteria (LSI, LSeI) [6].

3 Artificial neural network model

Neural networks are based on the concept of biological neurons. Artificial neurons process the signals using activation functions. The basic architecture of neural networks has been covered widely in previous studies done by Rumelhart in learning internal representation in parallel distributed processing [23], Lippmann in computation by neural networks [24], and Flood and Kartam in principles of neural networks in civil engineering [25]. The most widely and successfully used paradigm of neural network is feed forward backpropagation neural network [26].

In general, a neural network consists of an input layer, a hidden layer, and an output layer. The numbers of hidden layers used are rarely more than one [23, 24]. For the computation of target vectors, datasets are fed into the network as input vectors. The hidden layer and the output layer compute the target vectors by first multiplying the input by corresponding weights, adding the bias and then feeding the net value to the transfer function to get the output. The network is trained by several epochs for weights adjustment for minimizing the mean-squared error. Here, the error in

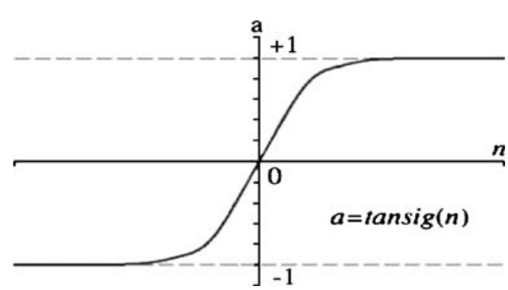

Fig. 4 Tangent sigmoid transfer function

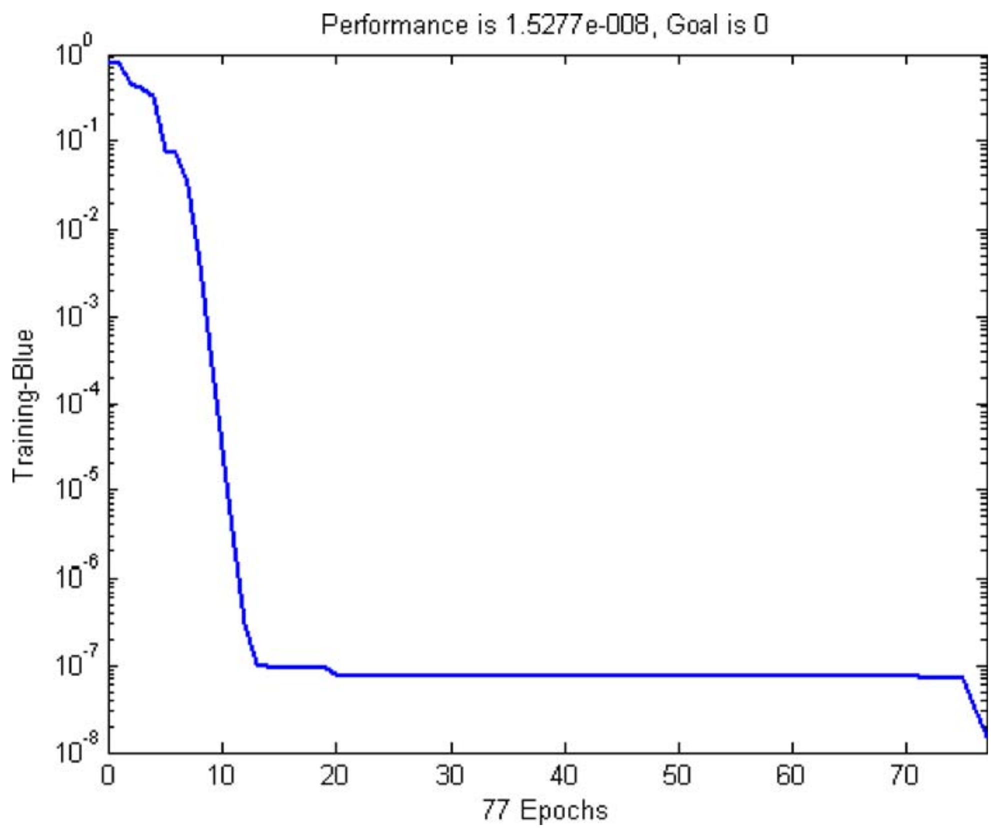

Fig. 5 Training curve for liquefaction susceptibility

weight propagates back in the network for adjustment. After the end of the training phase, the network should be able to predict the target vectors in the testing phase.

ANN models are capable of generalization. They can handle imprecise or deficient data and can capture nonlinear and complex interactions among variables of a system. Because of these strengths, ANN is emerging as a powerful tool for modeling.

3.1 Artificial neural network architecture

Both the networks used in this paper are feed forward backpropagation having only one hidden layer. MATLAB 7.0.1 has been used to define the network for predicting the liquefaction susceptibility and also for network to estimate CRR (Fig. 3). The weights for each layer are initialized during the start of the training phase with small values. If the weights are initialized with large values, it may so happen that the training may never converge to a fixed minimum mean-squared error. In this network, each layer has a weight matrix (W) corresponding to connections within the layer, a bias matrix (b) for that layer, and an activation function (f) for neurons. The activation function used in both networks is *hyperbolic tangent sigmoid* transfer function (Fig. 4).

Table 3 Details of network for CRR calculation

Network parameters	Value
No. of input vectors	3
No. of hidden layers	1
Neurons in layer 1	5
Neurons in layer 2	8
Neurons in output layer	1
Transfer function (in all three layers)	"tansig"
Learning rule	"learngdm"
Training function	"traingd"

Table 4 Details of network for prediction of liquefaction susceptibility

Network parameters	Value
No. of input vectors	4
No. of hidden layers	1
Neurons in layer 1	5
Neurons in layer 2	7
Neurons in output layer	1
Transfer function (in all three layers)	"tansig"
Learning rule	"learngdm"
Training function	"trainoss"

Table 5 Sensitivity value for each input channel

Sensitivity	BPNN
CSR	0.41407383
LSI	0.488402079
LSeI	0.348624046
CRR	0.447054823

The output of one layer becomes the new input value for the next layer and so on. Every neuron has a summer (Σ) which adds the biases with corresponding value obtained by multiplication of inputs and weights. Since every input parameter is connected to every neuron of the subsequent layer, it is common to have less number of parameters than neurons. The difference in the target value is calculated, and the error is propagated back into the network for required weight adjustment.

3.2 Data processing

In this study, the input parameters (Table 2) taken are CSR, LSeI, and LSI for the evaluation of CRR, and CRR, CSR, LSeI, and LSI for the prediction of liquefaction susceptibility. Among these parameters, the value of LSI varies over a wide range; thus, the network has to make large weight adjustments even for a small error in the target vector. For this reason, the values of LSI have to be normalized [−1 1]. Normalization can be accomplished for every input vector, p_i, of the dataset, which are divided by the maximum item of p_i, i.e.,

$$p_i/(p_i)_{max} \text{ or } (p_i - (p_i)_{min})/((p_i)_{max} - (p_i)_{min}) \tag{1}$$

This normalization method is selected to preprocess input vectors in estimating training vectors. Before introducing any new dataset for testing, normalization of the set has to be done. After the simulation of the network, the target vectors are converted back to their original units by postprocessing.

3.3 Learning rule

The learning rule defines the algorithm that is used to adjust the weights for the result to converge towards the target vector. Many rules have been developed by different authors, like the delta learning rule [27], Widrow–Hoff learning rule [28], and Winner-Take-All [29]. Here, the gradient descent with momentum rule has been applied to adjust weights and biases of the network in order to minimize the mean-squared error of the network. *Learngdm* calculates the weight change ($\mathrm{d}W$) for a given neuron from neurons input vector p_i and error (E). Following the relation for the weight adjustment:

$$\mathrm{d}W = \mathrm{mc} \times \mathrm{d}W^{\circ} + (1 - \mathrm{mc}) \times \mathrm{lr} \times \mathrm{gW} \tag{2}$$

Where, mc is the momentum constant, $\mathrm{d}W^{\circ}$ the previous $\mathrm{d}W$, lr the learning rate, and gW the previous gradient of weight change. The $\mathrm{d}W$ is backpropagated through the network until the derivative of error is available for the hidden layer.

3.4 Training

Training of a network refers to repeated application of input vectors to the network and calculation of error with respect to the target vectors. After every epoch, new weights and biases are calculated and fed back to the network for updating. This cycle repeats until the mean-squared error falls beneath a certain error goal or the maximum epochs are reached. Many training functions of MATLAB 7.0.1 like *traincgb* [30], *traincgf* [31], and *traindx* [32] were used to train the network. After many trials, it was observed that gradient descent and one step secant backpropagation training functions gave the least mean-squared error during the training phase for both the networks.

The training function used in the first network is *traingd*. A necessary condition for the application of gradient descent training function is that the input vectors, the transfer function, and the weights have their respective derivatives. Backpropagation is used to calculate derivatives of performance (perf) with respect

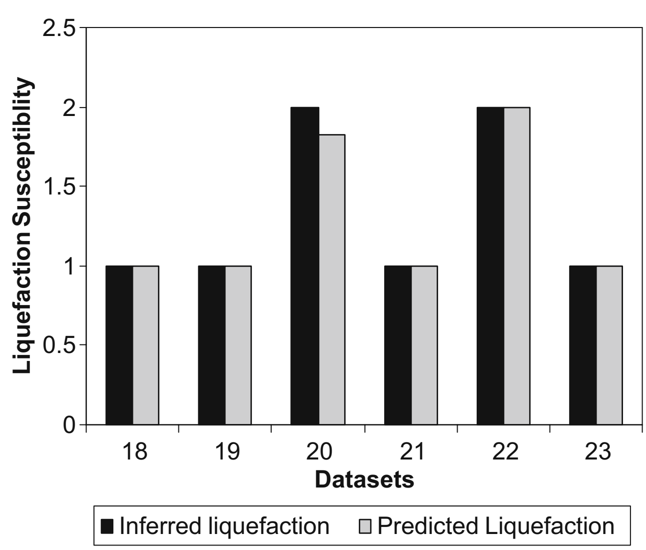

Fig. 6 Inferred vs. predicted liquefaction

to the weight and bias variables X. Each variable is adjusted according to gradient descent:

$$dX = \mathrm{lr} \times \mathrm{dperf}/dX \tag{3}$$

The training function used for the second network (Fig. 3), i.e., liquefaction prediction is one step secant back propagation training rule, *trainoss* [33]. A necessary condition for the application of *trainoss* function is that the input vectors, the transfer function, and the weights have their respective derivatives. The following formula is used for the correction of variables of network:

$$X = X + a \times dX; \tag{4}$$

where, dX is the search direction and X is the variable. For subsequent iterations, the search direction is calculated by the following formula:

$$dX = -\mathrm{gX} + \mathrm{Ac} \times \mathrm{X\_step} + \mathrm{Bc} \times \mathrm{dgX}; \tag{5}$$

where gX is the gradient, X_step is the change in the weights on the previous iteration, and dgX is the change in the gradient from the last iteration.

The training curve (Fig. 5) shows the progress of the training phase. The mean-squared error for the training phase is of the order 10^{-8}. In order to get the most accurate results, the number of layers, neurons in a layer, epochs, and learning rate were changed until the mean-squared error reached the error goal. Finally, all the elements of the network (Table 4) were fixed as tabulated in Table 2 for the first network and Table 3 for the second network.

4 Results and discussion

Liquefaction sensitivity index and liquefaction severity index are used to evaluate the severity from multi/hyperspectral satellite data [6]. The seismic demand and capacity on a soil layer are generally expressed in terms of CSR and CRR.

CRR, CSR, LSI, and LSeI values for the 17 locations of earthquake affected area in Bhuj region were calculated by following the standard procedures [14]. For the rest of the dataset, only LSI and LSeI were available. Using magnitude, distance and peak ground acceleration data on 2001 event CSR values were estimated [5]. The relation among these four variables was then used to predict CRR values by the BPNN technique. Following are the details about the networks used for evaluation of CRR (Table 3 and 4).

By using LSeI, LSI, CSR, and CRR (calculated) as input parameters for second BPNN, liquefaction susceptibility of different locations was predicted, and the accuracy of prediction is 99.99% for four out of five locations. An error of 40% is observed in one of the testing data. On the basis of this relation, the liquefaction susceptibility for the test of six locations is predicted.

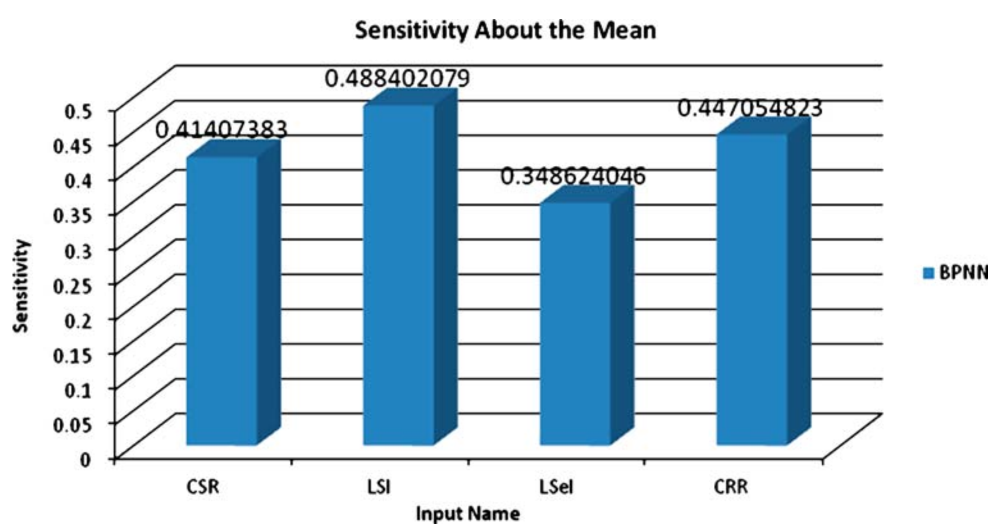

Fig. 7 Sensitivity vs. input parameters

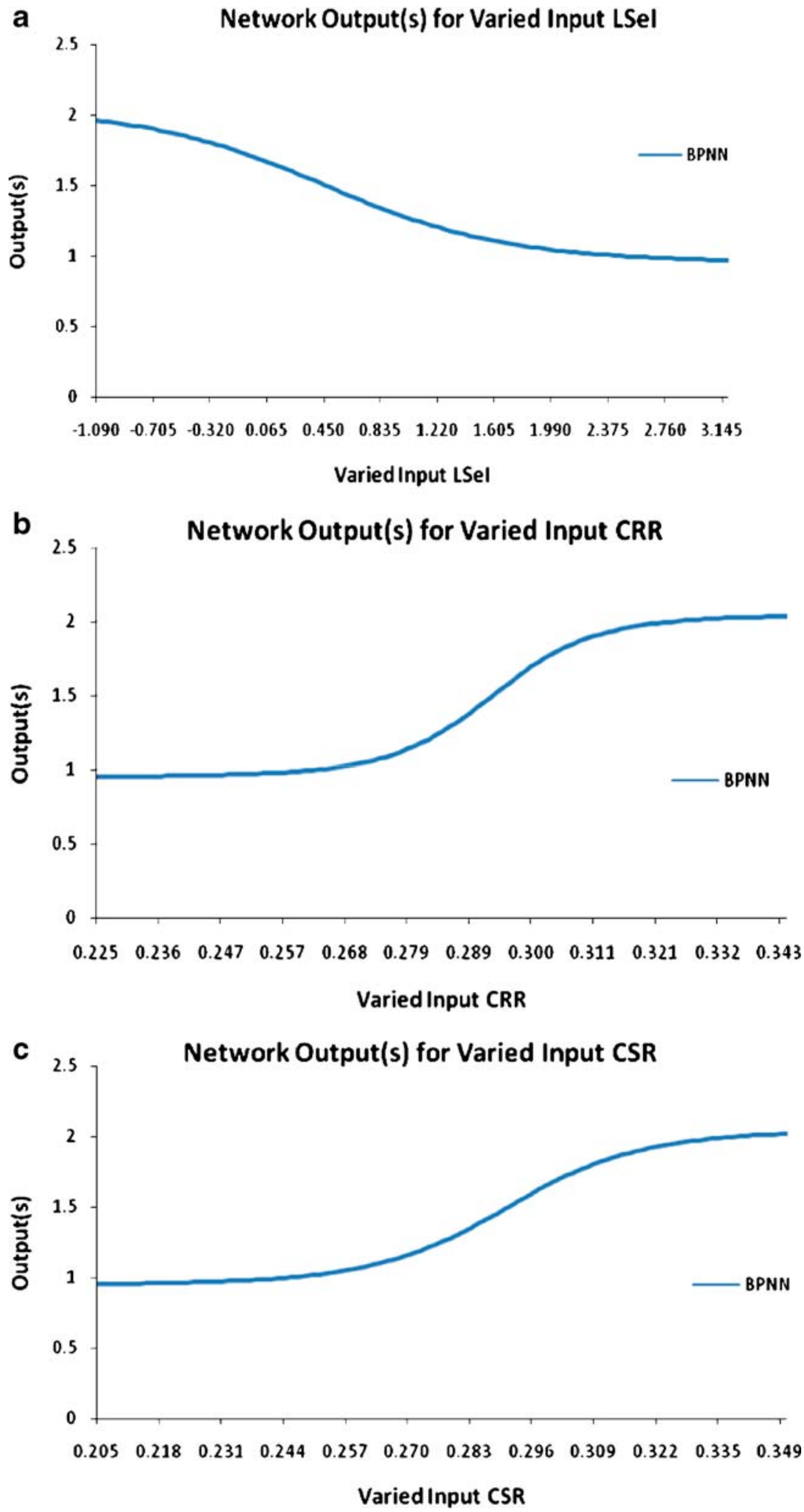

Fig. 8 **a** Network output(s) vs. varied input LSel. **b** Network output(s) vs. varied input CRR. **c** Network output(s) vs. varied input CRR. **d** Network output(s) vs. varied input CRR

Fig. 8 continued

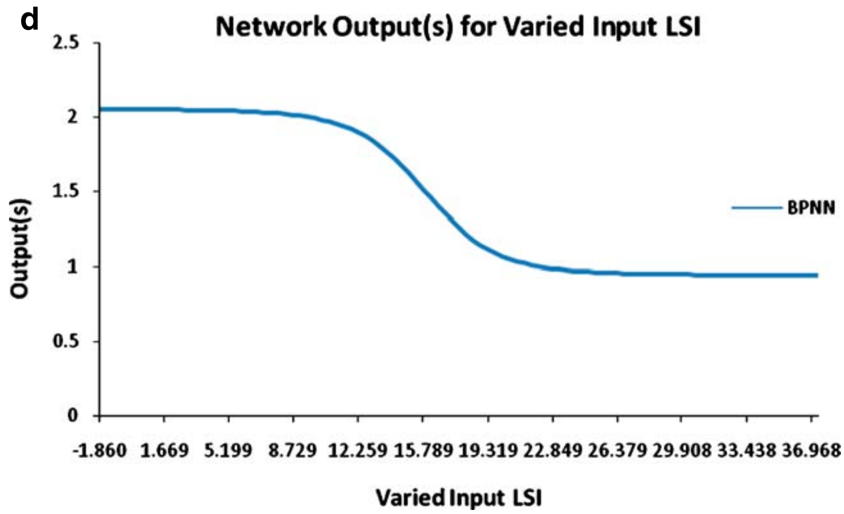

It is evident from Table 2 and Fig. 6 that the inferred and predicted liquefaction susceptibilities commensurate well. This again indicates that the network architecture has high degree of precision. Comparison between the inferred and predicted liquefaction susceptibilities (Fig. 6) indicates that the network architecture has high degree of precision.

5 Sensitivity analysis

Sensitivity analysis is a process for looking at the cause and effect relationship between the inputs and outputs of the dataset [34]. After training a neural network, it is important to know the effect that each of the network inputs individually on the network output. The basic concept is that each input channel to the network is varied slightly, and the corresponding change in the output(s) is reported. The input channel that produces high sensitivity values can be considered as significant and effective. The input channels which produce low sensitive values can be considered insignificant to the network and thus can be removed. This will reduce the size of the network, which in turn reduces the complexity and the training time. Moreover, this may also improve the network performance. Sensitive analysis about mean involves measure of the significance among the inputs of the neural model and defines how the model output varies in response to variation of an input. The first input is varied between its mean +/- a defined number of standard deviations while all other inputs are fixed at their respective means. The network output is computed for a defined number of steps above and below the mean (Table 5). This process is repeated for each input so that we can know the variation of each output with respect to the variation in each input (Fig. 8) for better utilization of dataset.

In the present study, LSI 0.488 (Fig. 7) provides the highest sensitivity, followed by CRR and CSR, with 0.447 and 0.414, respectively (Table 5). The lowest sensitivity is shown by LSel 0.348 (Fig. 8).

6 Conclusion

The study mainly focuses on predicting the liquefaction susceptibility of sediments in and around the Bhuj area based on the 2001 earthquake data. All 23 datasets characterizing the liquefaction susceptibility (CRR, CSR) and liquefaction severity (LSI, LSeI) were taken to train, test, and validate the ANN. The predicted relation among these variables is significant. Using the established relation, CRR values were predicted and then used subsequently for predicting the liquefaction susceptibility with 99% accuracy. This technique helps in the quick evaluation of liquefaction susceptibility using the LSI and LSeI.

References

1. Krinitzsky, E.L., Hynes, M.E.: The Bhuj, India earthquake: lessons learnt for earthquake safety of dams on alluvium. Eng. Geol. **58**, 193–202 (2002)
2. Ramakrishnan, D., Mohanty, K.K., Nayak, S.R.: Mapping the liquefaction induced soil moisture changes using remote sensing technique: an attempt to map the earth induced liquefaction around Bhuj, Gujarat, India. Geotech. Geolog. Eng. **24**, 1581–1602 (2006)
3. Singh, R., Roy, D., Jain, S.K.: Analysis of earth dams affected by the 2001 Bhuj Earthquake. Eng. Geol. **80**, 282–291 (2005)

4. Malik, J.N., Sohoni, P.S., Karanth, R.V., Merh, S.S.: Modern and historic seismicity of Kachchh Peninsula, Western India. J. Geol. Soc. India **54**, 545–550 (1999)
5. Sitharam, T.G., Govindaraju, L.: Geotechnical aspects and ground response studies in Bhuj earthquake, India. Geotech. Geolog. Eng. **22**, 439–455 (2004)
6. Ramakrishnan, D., Jeyaram, A., Mohanty, K.K., Nayak, S.R.: Mapping the liquefaction susceptible zones in parts of Kachchh region using IRS_WiFS and LISS-III data. In: Proceedings of the International Workshop on Earth System Process Related to Gujarat Earthquake Using Space Technology, pp. 27–29, 50–51. Department of Civil Engineering, IIT, Kanpur, India (2003)
7. Khandelwal, M., Roy, M.P., Singh, P.K.: Application of artificial neural network in mining industry. Indian Min. Eng. J. **43**(7), 19–23 (2004)
8. Goh, A.T.C.: Empirical design in geotechnics using neural networks. Geotechnique **45**(4), 709–714 (1995)
9. Goh, A.T.C.: Seismic liquefaction potential assessed by neural networks. J. Geotech. Geoenviron. Eng. **120**(9), 1467–1480 (1995)
10. Teh, C.L., Wong, K.S., Goh, A.T.C., Jaritngam, S.: Predicting settlement of shallow foundations using neural networks. J. Comput. Civ. Eng. **11**(2), 129–138 (1997)
11. Goh, A.T.C.: Neural network modeling of CPT seismic liquefaction data. J Geotech. Eng. **122**(1), 70–73 (1996)
12. Ural, D.N., Saka, H.: Liquefaction assessment by neural networks. Elect. J. Geotech. Eng. http://geotech.civen.okstate.edu/ejge/ppr9803/index.html (1998)
13. Hanna, M.A., Ural, D., Saygili, G.: Neural network model for liquefaction potential in soil deposits using Turkey and Taiwan earthquake data. Int. J. Soil Dyn. Earthqu. Eng. **27**(6), 521–540 (2007)
14. Ishihara, K.: Liquefaction and flow failure during earthquakes. Geotechnique **43**(3), 351–415 (1993)
15. Chu, B.-L., Hsu, S.-C., Chang, Y.-M.: Ground behavior and liquefaction analyses in central Taiwan-Wufeng. Eng. Geol. **71**, 119–139 (2003)
16. Lee, D.-H., Ku, C.-S., Yuan, H.: A study of the liquefaction risk potential at Yuanlin, Taiwan. Eng. Geol. 71, 97–117 (2003)
17. Yuan, H., Hiu Yang, S., Andrus, R.D., Hsein Juang, C.: Liquefaction induced ground failure: a study of the Chi-Chi earthquake cases. Eng. Geol. **17**, 141–155 (2003)
18. Seed, H.B., Tokimatsu, K., Harder, L.F., Chung, R.M.: The influence of SPT procedures in soil liquefaction resistance evaluations. J. Geotech. Eng., ASCE. **111**(12), 1425–1445 (1985), 16
19. Youd, T.L., Idriss, I.M., Andrus, R.D., Arango, I., Castro, G., Christian, J.T., Dobry, R., LiamFinn, W.D., Harder, L.F. Jr, Hynes, M.E., Ishihara, K., Koester, J.P., Laio, S.S.C., Marcuson, W.F. III, Martin, G.R., Mitchell, J.K., Moriwaki, Y., Power, M.S., Robertson, P.K., Seed, R.B., Stokoe, K.H. II: Liquefaction resistance of soils: summary report from the 1996 NCEER and 1998 NCEER/NSF workshops on evaluation of liquefaction resistance of soils. J. Geotech. Geoenviron. Eng. **127**(10), 817–833 (2001)
20. Seed, H.B., Idriss, I.M.: Simplified procedure for evaluating soil liquefaction potential. J. Soil Mech. Found Div., ASCE **97**(SM9), 1249–1273 (1971), 14
21. Seed, H.B., Idriss, I.M., Arango, I.: Evaluation of liquefaction potential using field performance data. J. Geotech. Eng. **109**, 458–482 (1983)
22. Youd, T.L., Perkins, D.M.: Mapping of liquefaction severity index. J. Geotech. Eng., ASCE. **113**(11), 1374–1392 (1987), 17
23. Rumelhart, D.E., Hinton, G.E., Williams, R.J.: Learning Internal Representation by Error Propagation in Parallel Distributed Processing. Massachusetts Institute of Technology Press, Cambridge (1986)
24. Lippmann, R.P.: An introduction to computing with neural nets. IEEE Trans. Acoust. Speech Signal Process. **42**, 4–22 (1987)
25. Flood, I., Kartam, N.: Neural networks in civil engineering. I: Principles and understanding. J. Comput. Civ. Eng., ASCE, **82**, 131–148 (1994)
26. Xia, Y.Y., Xie, Y.M., Zhu, R.G.: An engineering geology evaluation method based on an artificial neural network and its application. Eng. Geol. **47**, 149–156 (1997)
27. Rumelhart, D.E., McClelland, J.L.: Parallel Distributed Processing-Explorations in the Microstructure of Cognition 1/2. Massachusetts Institute of Technology Press, Cambridge (1986)
28. Widrow, B., Jovitz, M.C., Jacobi, G.T., Goldstein, G.: Generalization and information storage in networks of adaline neurons. In: Yovitz, M.C., Jacobi, G.T., Goldstein, G.D. (eds.) Self Organizing System, pp. 435–461. Spartan Books, Washington D.C. (1962)
29. Hecht-Neilsen, R.: Counterpropagation networks. Appl. Opt. **26**(23), 4979–4984 (1987)
30. Powell, M.J.D.: Restart procedures for the conjugate gradient method. Math. Program. **12**, 241–254 (1977)
31. Scales, L.E.: Introduction to Non-linear Optimization. Springer, New York (1985)
32. Gill, P.E., Murray, W., Wright, M.H.: Practical Optimization. Academic, New York (1981)
33. Battiti, R.: First and second order methods for learning; between steepest descent and Newton's method. Neural Comput. **4**(2), 141–166 (1992)
34. Singh, T.N., Verma, A.K., Sharma, P.K.: A neuro-genetic approach for prediction of time dependent deformational characteristic of rock and its sensitivity analysis. Geotech. Geolog. Eng. **25**, 395–407 (2007)